J. Fluid Mech. (1980), *vol.* 98, *part* 3, *pp.* 647–672
Printed in Great Britain

Comparison of nonlinear wave-resistance theories for a two-dimensional pressure distribution

By L. J. DOCTORS† AND G. DAGAN
School of Engineering, Tel-Aviv University, Israel

(Received 22 January 1979 and in revised form 22 October 1979)

The wave resistance of a two-dimensional pressure distribution which moves steadily over water of finite depth is computed with the aid of four approximate methods: (i) consistent small-amplitude perturbation expansion up to third order; (ii) continuous mapping by Guilloton's displacements; (iii) small-Froude-number Baba & Takekuma's approximation; and (iv) Ursell's theory of wave propagation as applied by Inui & Kajitani (1977). The results are compared, for three fixed Froude numbers, with the numerical computations of von Kerczek & Salvesen for a given smooth pressure patch. Nonlinear effects are quite large and it is found that (i) yields accurate results, that (ii) acts in the right direction, but quantitatively is not entirely satisfactory, that (iii) yields poor results and (iv) is quite accurate. The wave resistance is subsequently computed by (i)–(iv) for a broad range of Froude numbers. The perturbation theory is shown to break down at low Froude numbers for a blunter pressure profile. The Inui–Kajitani method is shown to be equivalent to a continuous mapping with a horizontal displacement roughly twice Guilloton's. The free-surface nonlinear effect results in an apparent shift of the first-order resistance curve, i.e. in a systematic change of the effective Froude number.

1. Introduction

The present study is concerned with the computation of wave resistance of bodies moving steadily in an inviscid fluid. The linearized approximation (thin-ship theory) is known to yield results which are in poor agreement with the experimental wave drag for bodies of practical shape. The need for better prediction has motivated the development of nonlinear methods whose application has been made possible by the advent of electronic computers. Although numerical solution of exact nonlinear equations might become feasible in the not-too-distant future, the emphasis at present is put on approximate nonlinear methods which still require a certain, but lesser, amount of numerical effort (for a detailed review see Wehausen 1973; see also the recent survey by Tulin 1979). Furthermore, such approximate methods may help to elucidate the main nonlinear mechanism governing the phenomenon which might be obscured by numerical solutions. It is customary at the present stage to check the accuracy of approximate methods by comparing the computed wave resistance with the residual drag of one or more models towed in laboratory tanks. Although the ultimate goal of any theory is to predict measured values satisfactorily, we feel that the many approximations involved in the aforementioned procedure preclude a

† L. J. Doctors is on leave from the School of Mechanical and Industrial Engineering, University of New South Wales, Kensington, NSW 2033, Australia.

0022–1120/80/4457–1260 $02.00

thorough evaluation of computational methods. Indeed, the measurement of residual drag implies the separation of the total drag into its components and, in spite of the refinements achieved in wave and wake surveys, there is still room for error and freedom of interpretation. Furthermore, it is known that viscous effects, which are disregarded in the theories we examine, can influence the wave drag. Finally, computation of wave resistance, even by approximate methods, involves elaborate computer programs which are difficult to check and may therefore contain additional errors.

An alternative approach which complements experiments, is the comparison of results based on approximate methods with those derived by numerical solution of the nonlinear equations of inviscid flow in simple cases. Such a solution has been presented recently by Salvesen & von Kerczek (1977) who have evaluated the wave resistance of a two-dimensional pressure distribution travelling on a free surface. This is a case sufficiently simple to avoid involved numerical work, but realistic enough to be of interest in applications such as air-cushion vehicles. The aim of the present study was to compute the wave resistance of the pressure distribution investigated by Salvesen & von Kerczek by a few existing theories and to compare results. The methods selected for examination here are: (i) the consistent small-amplitude perturbation theory up to third order, with the linearized theory as the first-order approximation; (ii) Guilloton's method in the interpretation of continuous mapping suggested by Noblesse & Dagan (1976); (iii) Baba & Takekuma's (1975) approximation of small-Froude-number flow, based on Ogilvie's (1968) work; and (iv) application of Ursell's (1960) theory of wave refraction to the computation of the wave pattern and wave resistance, as suggested by Inui & Kajitani (1977).

Method (i) is the classical theory of Stokes waves which has been applied to two-dimensional flows past bodies in water of infinite depth by Tuck (1965) and Salvesen (1969). Method (ii) has been developed in an intuitive way by Guilloton (1964) and has been applied in a rational way to evaluating wave resistance by Gadd (1973), who claims improved agreement with experiments in a few cases. Finally, the more recent methods (iii) and (iv) have also been found by their proponents to predict measured wave resistance of a few ship models better than the linearized theory.

Although the forementioned methods can be traced back in the references quoted above, a brief derivation of each of them is given in the sequel. This was found necessary because the case of a pressure acting on the free surface of a fluid of finite depth has not been considered explicitly in all cases, and also for the sake of completeness of the present study and for readers' ease.

2. Statement of the problem

We consider a two-dimensional pressure patch acting on the free surface of water of depth d and travelling to the right with a velocity c. The problem is made steady by imposing an equal and opposite velocity on the free stream, as shown in figure 1. A reference frame is defined with the x axis in the direction of motion and y is measured vertically upwards from the undisturbed free surface.

The usual assumptions that the fluid is incompressible, inviscid and lacks surface tension are made. The velocity may then be expressed as the sum of the uniform flow velocity $-c$ and the perturbation velocity with components u, v given by

$$u = \phi_x, \quad v = \phi_y, \tag{2.1}$$

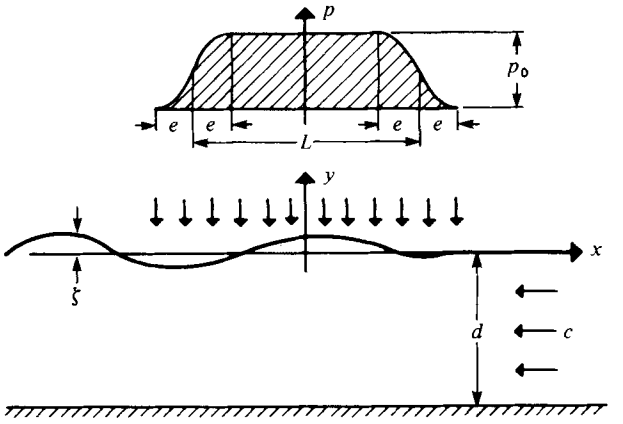

FIGURE 1. Definition of the problem and the pressure distribution.

where ϕ is the perturbation potential which must satisfy the Laplace equation

$$\nabla^2\phi = 0 \tag{2.2}$$

throughout the fluid region. In addition, as shown by Wehausen & Laitone (1960), for example, the dynamic condition

$$c\phi_x - \tfrac{1}{2}(\phi_x^2+\phi_y^2) - g\zeta = p/\rho \quad \text{on} \quad y = \zeta, \tag{2.3}$$

and the kinematic condition

$$\phi_y - (\phi_x - c)\,\zeta_x = 0 \quad \text{on} \quad y = \zeta \tag{2.4}$$

must also be satisfied on the free surface, whose elevation is $\zeta(x)$. Here $p(x)$ is the applied pressure, g is the acceleration of gravity and ρ is the water density. Eliminating ζ from (2.3) and (2.4) yields

$$\phi_y + \frac{1}{2g}[\nabla(\phi - cx)].\nabla[|\nabla(\phi - cx)|^2] + \phi_x h_x = ch_x \quad \text{on} \quad y = \zeta, \tag{2.5}$$

in which

$$h = p/\rho g. \tag{2.6}$$

Equation (2.5) can be used in lieu of (2.4), whereas (2.3) may serve to determine ζ.

In water of finite depth, the bed condition is required, namely

$$\phi_y = 0 \quad \text{on} \quad y = -d. \tag{2.7}$$

Finally, one needs to impose the well-known radiation condition, that waves must appear downstream of the disturbance.

In the next section, we consider various approximate solutions to the set of equations (2.1) to (2.4).

3. Derivation of approximate formulae

3.1. *Perturbation theory*

Chronologically, this was the earliest theory to be developed, and it has been applied by Salvesen & von Kerczek to the deep-water problem of a vortex (1976) and a pressure patch (1977). Here, the extension is made to the case of finite depth. It should be

pointed out that the higher-order terms for a Stokes wave are well known. However, the case of a pressure distribution in finite-depth water has not yet been examined.

We follow the procedure presented by Wehausen & Laitone for the solution of a free wave and expand the potential, the wave elevation, and the velocity in the following way:

$$\phi = \phi_1 + \phi_2 + \phi_3 + \ldots; \tag{3.1}$$

$$\zeta = \zeta_1 + \zeta_2 + \zeta_3 + \ldots; \tag{3.2}$$

$$c = c_0 + c_1 + c_2 + \ldots. \tag{3.3}$$

In the series, each term is considered to be smaller than the preceding one by the small parameter $\epsilon = p_0/\rho g L$, where p_0 is the nominal cushion pressure and L is the nominal length of the patch. An interesting feature of the perturbation scheme is that it provides both corrections to the flow ((3.1) and (3.2)) *and* a correction to the velocity (3.3) – implying that in general one cannot specify the speed explicitly. (It is remembered that the actual velocity of the disturbance is c, while c_0 is merely a computational artifact.)

These expressions are now substituted into (2.2) to (2.4) and terms of the same order of magnitude are collected. After some algebra, one obtains:

$$\nabla^2 \phi_i = 0 \tag{3.4}$$

for the continuity equation;

$$\left.\begin{aligned} &\phi_{1y} + c_0 \zeta_{1x} = 0, \\ &\phi_{2y} + c_0 \zeta_{2x} = -\zeta_1 \phi_{1yy} + \phi_{1x}\zeta_{1x} - c_1 \zeta_{1x}, \\ &\phi_{3y} + c_0 \zeta_{3x} = -\phi_{1yy}\zeta_2 - \phi_{2yy}\zeta_1 - \tfrac{1}{2}\phi_{1yyy}\zeta_1^2 \\ &\qquad + \phi_{1x}\zeta_{2x} + \phi_{2x}\zeta_{1x} + \phi_{1xy}\zeta_1\zeta_{1x} - c_1\zeta_{2x} - c_2\zeta_{1x}, \end{aligned}\right\} \tag{3.5}$$

for the kinematic condition;

$$\left.\begin{aligned} &c_0\phi_{1x} - g\zeta_1 = p/\rho, \\ &c_0\phi_{2x} - g\zeta_2 = -c_0\phi_{1xy}\zeta_1 - c_1\phi_{1x} + \tfrac{1}{2}\phi_{1x}^2 + \tfrac{1}{2}\phi_{1y}^2, \\ &c_0\phi_{3x} - g\zeta_3 = -c_0(\phi_{1xy}\zeta_2 + \phi_{2xy}\zeta_1 + \tfrac{1}{2}\phi_{1xyy}\zeta_1^2) - c_2\phi_{1x} \\ &\qquad + \phi_{1x}\phi_{2x} + \phi_{1y}\phi_{2y} + \zeta_1(\phi_{1x}\phi_{1xy} + \phi_{1y}\phi_{1yy}) - c_1(\phi_{2x} + \phi_{1xy}\zeta_1), \end{aligned}\right\} \tag{3.6}$$

for the dynamic condition; and

$$\phi_{iy} = 0 \quad \text{on} \quad z = -d \tag{3.7}$$

for the bed condition.

These equations are the same as those in Wehausen & Laitone, except that two typographical errors in the signs in their equation (27.7) have been corrected in (3.6c).

The free-surface elevation ζ_i may be eliminated from (3.3) and (3.6) to yield the combined free-surface condition

$$\phi_{ixx} + k_0 \phi_{iy} = \frac{1}{\rho c_0} p_{ix}, \tag{3.8}$$

where $k_0 = g/c_0^2$ is the fundamental wavenumber.

Thus, the higher-order solutions ($i = 2, 3, \ldots$) resemble the well-known first-order solution:

$$\phi_i(x, y) = \frac{1}{\pi\rho c}\left[\int_0^\infty \frac{\cosh[k(y+d)]\, S_i(x,k)}{\cosh(kd)\, q(k)}\, dk - \frac{\pi \cosh[k_1(y+d)]\, C_i(x,k_1)}{\cosh(k_1 d)\, r(k_1)}\right], \tag{3.9}$$

where
$$C_i(x,k)+iS_i(x,k) = \int p_i(s)\exp[ik(x-s)]\,ds, \tag{3.10}$$

and k_1 is the non-zero solution of

$$q(k) = k - k_0\tanh(kd) = 0 \tag{3.11}$$

and
$$r(k) = q'(k) = 1 - k_0 d\,\mathrm{sech}^2(kd). \tag{3.12}$$

When $k_0 d < 1$ (the supercritical condition), there is no non-zero solution of (3.11), and the second term in (3.9) is zero. For simplicity, the 1 subscript in k_1 will now be dropped.

Each of the p_i induces a downstream wave of amplitude A_i and phase angle α_i, which follow from (3.10). The result is

$$A_i e^{i\alpha_i} = -\frac{2ik}{\rho g r}[C_i(0,k)+iS_i(0,k)]. \tag{3.13}$$

The first-order pressure is simply

$$p_1 = p, \tag{3.14}$$

and this yields a wave profile and potential far downstream of the form

$$\zeta_1 = A_1\cos(kx+\alpha_1), \tag{3.15}$$

and
$$\phi_1 = c_0 A_1 \frac{\cosh[k(y+d)]}{\sinh(kd)}\sin(kx+\alpha_1). \tag{3.16}$$

The second-order pressure may be obtained by eliminating ζ_2 from (3.5*b*) and (3.6*b*). It is necessary to put

$$c_1 = 0 \tag{3.17}$$

in order to prevent ζ_2 from becoming unbounded downstream. The second-order pressure is then found to be

$$p_2 = \rho[c_0\zeta_1(k_0\phi_{1x}-\phi_{1xy})+\tfrac{1}{2}(\phi_{1x}^2+\phi_{1y}^2)], \tag{3.18}$$

which yields a trailing wave profile of the form

$$\zeta_2 = A_2\cos(kx+\alpha_2)+kA_1^2\left\{\frac{\cosh(kd)\,[2\cosh^2(kd)+1]\cos[2(kx+\alpha_1)]}{4\sinh^3(kd)}-\frac{1}{2\sinh(2kd)}\right\} \tag{3.19}$$

and

$$\phi_2 = c_0 A_2\frac{\cosh[k(y+d)]}{\sinh(kd)}\sin(kx+\alpha_2)+3c_0kA_1^2\frac{\cosh[2k(y+d)]}{8\sinh^4(kd)}\sin[2(kx+\alpha_1)]. \tag{3.20}$$

Finally, the third-order pressure is found from (3.5*c*) and (3.6*c*). A bounded solution for ϕ_3 is obtained when

$$c_2 = c_0 k^2 A_1^2\left\{\frac{9+8\sinh^2(kd)+8\sinh^4(kd)}{16\sinh^4(kd)}-\frac{1}{8\sinh^2(kd)\cosh^2(kd)}\right\}. \tag{3.21}$$

This expression differs from the usual one for the velocity correction for Stokes waves in water of finite depth. The difference is the inclusion here of the second term in (3.21) which results from the mean depression of the trailing wave profile in (3.19). (The depth d is that measured upstream.)

The results for the third-order pressure, and the downstream wave profile and potential are:

$$\begin{aligned} p_3 = \rho[&c_0 k_0(\phi_{1x}\zeta_2 + \phi_{2x}\zeta_1 + \tfrac{1}{2}\phi_{1xy}\zeta_1^2 - c_2\zeta_1) \\ &- c_0(\phi_{1xy}\zeta_2 + \phi_{2xy}\zeta_1 + \tfrac{1}{2}\phi_{1xyy}\zeta_1^2) \\ &- c_2\phi_{1x} + \phi_{1x}\phi_{2x} + \phi_{1y}\phi_{2y} + \zeta_1(\phi_{1x}\phi_{1xy} + \phi_{1y}\phi_{1yy})]; \end{aligned} \tag{3.22}$$

$$\begin{aligned} \zeta_3 = {} & A_3\cos(kx+\alpha_3) \\ & + kA_1A_2\left\{\frac{3+4\sinh^2(kd)+2\sinh^4(kd)}{2\cosh(kd)\sinh^3(kd)}\cos(kx+\alpha_1)\cos(kx+\alpha_2)\right. \\ & \left. - \frac{3+6\sinh^2(kd)+2\sinh^4(kd)}{2\cosh(kd)\sinh^3(kd)}\sin(kx+\alpha_1)\sin(kx+\alpha_2)\right\} \\ & + k^2A_1^3\left\{\frac{3[8\cosh^6(kd)+1]}{64\sinh^6(kd)}\cos[3(kx+\alpha_1)]\right. \\ & \left. + \frac{3+15\sinh^2(kd)+12\sinh^4(kd)+2\sinh^6(kd)}{16\sinh^4(kd)\cosh^2(kd)}\cos(kx+\alpha_1)\right\}; \end{aligned} \tag{3.23}$$

and

$$\begin{aligned} \phi_3 = {} & c_0A_3\frac{\cosh[k(y+d)]}{\sinh(kd)}\sin(kx+\alpha_3) \\ & + 3c_0kA_1A_2\frac{\cosh[2k(y+d)]}{4\sinh^4(kd)}\sin(2kx+\alpha_1+\alpha_2) \\ & + c_0k^2A_1^3\frac{[9-4\sinh^2(kd)\cosh[3k(y+d)]}{64\sinh^7(kd)}\sin[3(kx+\alpha_1)]. \end{aligned} \tag{3.24}$$

The wave resistance may be obtained in the usual way by means of a control surface surrounding the disturbance. The result for the resistance per unit width is

$$R = \tfrac{1}{2}\rho g\zeta^2 + \frac{1}{2}\int_{-d}^{\zeta}(\phi_y^2 - \phi_x^2)\,dy,$$

the integration being performed at any station downstream of the pressure p. It is then necessary to substitute (3.15), (3.16), (3.19), (3.20), (3.23) and (3.24). Care must be taken to retain the required number of terms of each stage of the algebra, which is rather lengthy and prone to error. The contributions to the first three orders of resistance are found to be

$$\left.\begin{aligned} R_1 &= \tfrac{1}{4}\rho g r A_1^2, \\ R_2 &= \tfrac{1}{2}\rho g r A_1A_2\cos(\alpha_1-\alpha_2), \\ R_3 &= \tfrac{1}{4}\rho g r\left\{A_2^2 + 2A_1A_3\cos(\alpha_1-\alpha_3) + \frac{k^2A_1^4}{16r\sinh^6(kd)\cosh^2(kd)}\right. \\ &\quad \left.\times[9-9k_0d+18\sinh^2(kd)+39\sinh^4(kd)+12\sinh^6(kd)-8\sinh^8(kd)]\right\}. \end{aligned}\right\} \tag{3.25}$$

Because the pressures p_2 and p_3 extend infinitely far downstream, it was found easier to use the following formula instead:

$$R_i = \int p_1\zeta_{ix}\,dx. \tag{3.26}$$

Here the integration is carried out numerically over the length of the (first-order) pressure distribution. For the purpose of calculating ζ_i in this range, it is permissible to truncate the p_2 and p_3 distributions.

3.2. *Continuous-mapping theory (Guilloton's method)*

Guilloton's method has been given a rational derivation with the aid of the general concept of continuous mapping by Noblesse & Dagan (1976). Since the presence of the pressure on the free-surface was not handled before and also for the sake of completeness the main points are given again here.

The flow domain (for infinite depth) beneath $y = \zeta$ is continuously mapped onto the lower half-plane X, Y by

$$x = X + \xi(X, Y), \quad y = Y + \eta(X, Y), \tag{3.27}$$

such that

$$\eta(X, 0) \equiv \zeta(x) \tag{3.28}$$

and

$$u(X, Y) \equiv u(x, y), \quad v(X, Y) \equiv v(x, y). \tag{3.29}$$

Under these transformations the free-surface conditions (2.3) and (2.4) become

$$cu - \tfrac{1}{2}(u^2 + v^2) - g\eta = g\chi \quad \text{on} \quad Y = 0 \tag{3.30}$$

and

$$v(1 + \xi_X) - (u - c)\,\eta_X = 0 \quad \text{on} \quad Y = 0, \tag{3.31}$$

where

$$\chi(X, 0) \equiv h(x) \tag{3.32}$$

is the 'transformed pressure' in the reference domain and corresponds to the 'linearized hull' in Guilloton's terminology. The continuity and irrotationality conditions satisfied by $\mathbf{u}$ can be written down in terms of X and Y using (3.27) and chain differentiation. Subsequently, both velocity and mapping are expanded in small perturbation series

$$u = u_1 + u_2 + \ldots; \quad v = v_1 + v_2 + \ldots; \quad \xi = \xi_1 + \xi_2 + \ldots; \quad \eta = \eta_1 + \eta_2 + \ldots. \tag{3.33}$$

We substitute in (3.27) to (3.31) and the field equations, to obtain at first order

$$u_1 = \Phi_{1X}, \quad v_1 = \Phi_{1Y}, \quad \Phi_{1XX} + \Phi_{1YY} = 0 \quad \text{for} \quad Y \leqslant 0, \tag{3.34}$$

and

$$v_1 + c\eta_{1X} = 0 \quad \text{on} \quad Y = 0, \tag{3.35}$$

$$cu_1 - g\eta_1 = g\chi \quad \text{on} \quad Y = 0, \tag{3.36}$$

which is identical to the first-order problem of the previous section (3.5), (3.6), except for replacing h by χ and ϕ_1 by Φ_1.

Following Noblesse & Dagan (1976), the second-order velocity field is represented as

$$u_2 = -u_1\xi_{1X} - v_1\eta_{1X} + \theta_{2X}, \tag{3.37}$$

and

$$v_2 = -u_1\xi_{1Y} - v_1\eta_{1Y} + \theta_{2Y}, \tag{3.38}$$

such that $\mathbf{u}_2$ satisfies the irrotationality condition but not the continuity equation. The latter and free-surface condition (3.30), (3.31) yield for the pseudo-potential θ_2:

$$\theta_{2XX} + \theta_{2YY} = \nabla^2(\xi_1 u_1 + \eta_1 v_1) \quad \text{for} \quad Y \leqslant 0, \tag{3.39}$$

and

$$\theta_{2XX} + k_0\theta_Y = u_1(\xi_{1XX} + k_0\xi_{1Y}) + v_1(\eta_{1XX} + k_0\eta_{1Y}) + (\xi_{1X} + u_1/c)\,(u_{1X} - k_0 v_1) \quad \text{on} \quad Y = 0, \tag{3.40}$$

while

$$g\eta_2 = cu_2 - \tfrac{1}{2}(u_1^2 + v_1^2) \quad \text{on} \quad Y = 0. \tag{3.41}$$

Up to this point, the mapping ξ_1, η_1 is arbitrary except for (3.28). Guilloton's mapping was shown to be the particular one which is harmonic and cancels identically the non-homogeneous term on the right-hand side of (3.40). In the absence of χ the mapping turns out to be

$$\xi_1^G - \Phi_1/c, \quad \eta_1^G = cu_1/g. \tag{3.42}$$

Guilloton's approximation consists in neglecting also the right-hand side of (3.39), which becomes, for $\chi = 0$,

$$\theta_{2XX} + \theta_{2YY} = -\frac{1}{c}(u_1^2 + v_1^2)_X, \tag{3.43}$$

so that $\theta_2 \equiv 0$ and then the wave resistance at second order is expressed simply with the aid of the far free waves of the linearized first-order potential Φ_1. This recipe has to be modified, however, when a pressure is present. In line with Guilloton's mapping we select here

$$\xi_1 = \xi_1^G = -\frac{\Phi_1}{c}, \quad \eta_1 = \frac{cu_1}{g} - \chi, \tag{3.44}$$

such that (3.36) is satisfied and (3.44) degenerates into (3.42) for $\chi \equiv 0$, but the extension of χ beneath $Y = 0$ is left unspecified at present. Substituting (3.44) into (3.39) and (3.40) yields

$$\theta_{2XX} + \theta_{2YY} = -\frac{1}{c}(u_1^2 + v_1^2)_X - \nabla^2(\chi v_1) \quad \text{for} \quad Y \leqslant 0, \tag{3.45}$$

and

$$\theta_{2XX} + k_0\theta_{2Y} = -k_0(u_1\chi_X + v_1\chi_Y) \quad \text{for} \quad Y = 0. \tag{3.46}$$

It is seen that there is no way to extend χ such as to cancel both the last term of (3.45) and the right-hand side of (3.46) as in Guilloton's procedure. We have decided to extend χ such as to satisfy the first requirement, i.e.

$$\nabla^2(\chi v_1) = 0, \tag{3.47}$$

which, together with (3.32), defines χ uniquely by

$$\chi(X, Y) = \frac{1}{v_1}\operatorname{Re}\frac{i}{\pi}\int_{-\infty}^{\infty}\frac{\chi(s,0)\,v_1(s,0)}{s - X - iY}\,ds, \tag{3.48}$$

and, after substituting in (3.40), gives

$$\theta_{2XX} + k_0\theta_{2Y} = -k_0(\chi u_1)_X + \frac{k_0}{\pi}\int_{-\infty}^{\infty}\frac{[\chi(s,0)\,v_1(s,0)]_s}{s - X}\,ds \quad \text{on} \quad Y = 0. \tag{3.49}$$

In line with Guilloton's method we also neglect the remaining part of the right-hand side of (3.45) so that θ_2 is a harmonic function determined by (3.49).

The wave resistance now is obtained with the aid of the free waves associated with the total potential $\Phi_1 + \theta_2$, which is uniquely determined.

Summarizing the preceding derivations, the computation of the wave resistance generated by a pressure patch $h(x)$ requires solving the linearized problem for the transformed distribution $\chi(X)$, which is obtained from $h(x)$ by the horizontal straining ξ_1 [(3.32) and (3.42)]. Since ξ_1 depends on the solution, an iterative procedure which starts with $\xi_1 = 0$, $\chi = h$ as a first approximation is indicated. Subsequently, θ_2 is computed from (3.49) and the amplitude of the far free waves and the wave resistance associated with $\Phi_1 + \theta_2$ are easily found as in (3.25a).

In the case of water of finite depth the vertical mapping (3.44) will generally be different from zero on the line $Y = -d$ in the reference domain, unless we supplement (3.47) with an additional condition for χ on $Y = -d$. Such a condition has not been considered here and we have disregarded the influence of bottom distortion when applying the method to finite depth.

It should be mentioned that other mapping procedures, that is, methods for extending χ below the free surface, are possible. In addition to the one given by (3.47) the following was also tested:

$$\nabla^2\chi = 0.$$

As it turned out, the results were almost identical to those displayed in figure 3 (where (3.47) was satisfied). Thus, the details of the mapping procedure are unimportant – at least for the range of data used here.

3.3. *Small-Froude-number approximation (Baba & Takekuma's approximation)*

A small-Froude-number approximation has been suggested for two-dimensional flows by Ogilvie (1968) and a succinct derivation for the three-dimensional case was given by Newman (1976). Following the last reference for the case at hand, the perturbation potential is represented as

$$\phi = \phi_0 + \phi_1, \tag{3.50}$$

where $-cx + \phi_0$ is the zero-Froude-number solution, obtained from (2.1) to (2.4) by keeping c fixed while $c^2/g \to 0$. Furthermore, it is assumed that $\phi_1 = O(c^4/g^2)$ while by differentiation $\partial^{m+n}\phi_1/\partial x^m \partial y^n = O[(c^2/g)^{2-m-n}]$, an ordering which is suggested by the behaviour of the potential of the far free waves (3.16). In contrast, ϕ_0 and its derivatives at any order are $O(1)$. Substituting (3.50) into (2.3) yields for the free-surface elevation

$$\zeta = \zeta_0 + \zeta_1,$$

where
$$\zeta_0 = -h + \frac{1}{g}[c\phi_{0x} - \tfrac{1}{2}(\phi_{0x}^2 + \phi_{0y}^2)] + O(c^6/g^3),$$

and
$$\zeta_1 = \frac{c}{g}\phi_{1x} - \frac{1}{g}(\phi_{0x}\phi_{1x} + \phi_{0y}\phi_{1y}) + O(c^6/g^3). \tag{3.51}$$

Substituting (3.50) and (3.51) into (2.1), (2.5) and (2.7) yields the following sequence of equations for ϕ_0 and ϕ_1 at $O(1)$ and $O(c^2/g)$, respectively:

$$\nabla^2\phi_0 = 0, \tag{3.52}$$

$$\phi_{0y} + \phi_{0x}h_x = ch_x \quad \text{on} \quad y = -h, \tag{3.53}$$

and
$$\phi_{0y} = 0 \quad \text{on} \quad y = -d; \tag{3.54}$$

$$\nabla^2\phi_1 = 0, \tag{3.55}$$

$$\phi_{1y} + \frac{1}{g}[(\phi_{0x} - c)^2\phi_{1xx} + 2(\phi_{0x} - c)\phi_{0y}\phi_{1xy} + \phi_{0y}^2\phi_{1yy}] + \phi_{1x}h_x$$
$$= -\frac{1}{g}[(\phi_{0x} - c)^2\phi_{0xx} + 2(\phi_{0x} - c)\phi_{0y}\phi_{0xy} + \phi_{0y}^2\phi_{0yy}] - (\zeta_0 + h)(\phi_{0yy} + h_x\phi_{0xy})$$
$$\text{on} \quad y = \zeta_0 \tag{3.56}$$

and
$$\phi_{1y} = 0 \quad \text{on} \quad y = -d. \tag{3.57}$$

In (3.56) ϕ_0 is evaluated on $y = -h$, whereas ϕ_1 is defined on $y = \zeta_0$, and the last term originates from the corresponding Taylor expansion in the y direction. In the absence of a pressure on the free surface ($h = 0$), (3.53) degenerates into the rigid-wall condition and (3.56) attains the simple form presented by Ogilvie (1968) and Newman (1976). Furthermore, they assume that at the same order it is permitted to transfer (3.56) from $y = \zeta_0$ to $y = -h$ (that is, $y = 0$ for zero pressure). Even for $h = 0$, (3.56) is still quite complicated and Baba & Takekuma (1975) have suggested a further simplification, namely to linearize (3.56) by replacing the left-hand side by $\phi_{1y} + (c^2/g)\,\phi_{1xx}$. Hence, in Baba & Takekuma's approximation, the nonlinearity of the free-surface condition is manifested in the presence of an effective pressure acting on $y = 0$, represented by the right-hand side of (3.56) for $h = 0$.

In the present case we take advantage of the fact that, for the pressure patch under consideration (see § 4), $h/L \ll 1$ and $h_x \ll 1$. We set $\phi_0 = \phi_{01} + \phi_{02}$ with $\phi_{01} = O(h)$, $\phi_{02} = O(h^2)$ and neglect terms of $O(h^3)$. Equation (3.53) now yields

$$\phi_{01y} = ch_x \quad \text{on} \quad y = 0 \tag{3.58}$$

and

$$\phi_{02y} = -(h\phi_{01x})_x \quad \text{on} \quad y = 0, \tag{3.59}$$

while ϕ_{01} and ϕ_{02} also satisfy (3.52) and (3.54). As for ϕ_1, (3.56) leads under Baba & Takekuma's linearization and the above expansion of ϕ_0 to the following free-surface condition for $\phi = \phi_{01} + \phi_{02} + \phi_1$:

$$\phi_{xx} + k_0\phi_y = gH_x/c \quad \text{on} \quad y = 0, \tag{3.60}$$

where

$$H = h - \frac{h\phi_{01x}}{c} + \frac{1}{k_0}\left(hh_{xx} + \tfrac{1}{2}h_x^2 + \frac{3}{2c^2}\phi_{01x}^2\right). \tag{3.61}$$

Thus we see that the boundary condition on the actual free surface has been shifted to the line $y = 0$. This can be done if h is small compared to λ, the wavelength of the free waves. Now

$$h/\lambda = \frac{h}{2\pi c^2/g} = \frac{1}{2\pi}\frac{h}{L}\frac{1}{F^2},$$

and its maximum value of 0·013 occurs when $h/L = 0{\cdot}02$ and $F = 0{\cdot}5$ (for the range of numerical values examined). Hence this approximation seems to be justified. Of course, it must be acknowledged that at lower Froude numbers, or higher pressures, this simplification would not be valid.

Hence, with Baba & Takekuma's approximation and the assumption of small h_x, determining ϕ has been reduced to solving the linearized free-surface problem (3.60) in which the effective pressure is expressed in terms of the actual pressure h and the small-Froude-number solution ϕ_{01} (3.58) up to order h^2. It is easy to ascertain that the same equation (3.60) could be obtained from the consistent perturbation expansion by summing up the first- and second-order equations in (3.8), by replacing ϕ_1 and ϕ_{1y} by ϕ_{01} and h_x, respectively, and neglecting terms of order (c^4/g^2) or higher. In other words, (3.60) and (3.61) can be obtained by a double expansion process for small amplitude and small Froude number up to terms of order $(h/L)^2$ and c^2/gL in a manner considered in a previous paper for submerged bodies by Dagan (1972). The wave resistance can be obtained from the amplitude of the far free waves (3.15) in which p is replaced by ρgH or by integration along ζ_1 (3.51) as in (3.26). The problem is reduced, therefore, to solving first the Neumann problem for ϕ_{01} (3.58) and subsequently the linearized wave problem for ϕ ((3.60) and (3.61)).

3.4. *Inui–Kajitani approximation based on Ursell's theory*

Inui & Kajitani (1977) have applied Ursell's theory of refraction of Kelvin waves generated by a pressure point which travels on a non-uniform current in the horizontal plane. It is assumed that the waves are of small amplitude and only the first-order term is retained, and that the current vertical velocity is negligible. Ursell's theory is essentially a kinematical one in the sense that the refraction pattern is determined with the aid of the law of conservation of the wavenumber while the amplitude change is not considered.

Inui & Kajitani (1977) assumed that, in the case of waves generated by a ship hull, the non-uniform current is represented by the velocity field of the double model (i.e. zero Froude number or, equivalently, rigid-wall free-surface condition) and, therefore, their method applies to moderate or small Froude numbers. Furthermore, it is assumed that the strength of the sources which generate the body shape in the rigid-wall approximation is the one appearing in the potential of the free waves, modified by a factor representing the refraction effect. In other words, the nonlinearity of the free-surface condition manifests itself in phase shifts of the wave system generated by the hull.

In the present case of a two-dimensional flow, the theory is considerably simplified. The starting point is the representation of the potential of a free wave of unit amplitude in deep water as

$$\phi_w = \exp\left[k_0(|\psi_x|\, y + i\psi)\right], \tag{3.62}$$

where ψ is the phase function ($\psi \equiv x$ for uniform current) and $y = 0$ represents the free surface in the absence of waves. The function ϕ_w satisfies the Laplace equation near $y = 0$ only approximately at the lowest order in the Froude number, i.e. at order $(g/c^2)^2$, while terms of order g/c^2 and higher are neglected. The phase function ψ is subsequently determined by substituting ϕ_w in the free-surface condition (3.56) which becomes, for flow under a rigid wall, i.e. for zero values of h, ζ_0 and $\phi_{0,y}$:

$$g\phi_y + (\phi_{0x} - c)^2 \phi_{xx} = 0 \quad \text{on} \quad y = 0, \tag{3.63}$$

where $\phi = \phi_0 + \phi_1$ is the total disturbance potential. Hence, from (3.62) and (3.63) we have, again, at the lowest order in (c^2/g):

$$\psi_x = 1/(\phi_{0x}/c - 1)^2 \tag{3.64}$$

which expresses the phase function in terms of the zero-Froude-number solution. In the present case (3.64) is valid strictly speaking behind the pressure patch, where the rigid-wall solution applies, but, for small $h/L = p/\rho g L$, (3.64) is a good approximation even along the pressure distribution. The justification for this statement is essentially the same as that given in § 3.3, where it was shown that the depression caused by the pressure is small compared to the wavelength.

In line with Inui & Kajitani's assumption, we now write the potential of the free waves generated by the pressure patch as a superposition of free waves of amplitude given by the linearized theory for uniform flow (see equation (3.15)), but with the phase of (3.64). Hence, the far free-surface profile is given by

$$\zeta(x) = -2\,\mathrm{Re}\int h_s \exp\left[ig\int_s^x \frac{d\sigma}{(\phi_{0\sigma} - c)^2}\right] ds \quad \text{for} \quad x \to -\infty. \tag{3.65}$$

For $x \to -\infty$, $\phi_{0\sigma} \to 0$ and $\zeta(x)$ degenerates into a simple harmonic wave so that the wave resistance can be computed as in § 3.1.

Hence, computing the wave resistance first requires solving for the zero-Froude-number flow and deriving $\phi_0(x, 0)$ and subsequently computing A from (3.65) by two quadratures. The profile (3.65) can be regarded as a summation of elementary waves generated by pressure elements $p\,ds$ whose phase is modified by the presence of the current of velocity $\phi_{0x} - c$. Obviously, for uniform current ($\phi_{0x} = 0$), (3.65) degenerates into the first-order perturbation solution.

For small h/L and h_x, as presumed here, we may write

$$\frac{1}{(\phi_{0x}/c - 1)^2} = 1 + \frac{2\phi_{01x}}{c} + O(h^2), \tag{3.66}$$

where ϕ_{01} satisfies (3.58). Hence, for large negative x, $\phi_{01} \to 0$, and the phase function ψ given by (3.64) becomes

$$\psi(x - s) = x - s - \frac{2\phi_{01}(s, 0)}{c}. \tag{3.67}$$

Substitution of (3.67) into (3.65) yields the following result for the downstream complex wave amplitude:

$$A = -2\int h_s \exp\{-ik_0[s + (2/c)\,\phi_{01}(s, 0)]\}\,ds, \tag{3.68}$$

from which the wave resistance can be obtained.

A point of considerable interest discovered during the computation process is that by the change of variable,

$$\mu = x + (2/c)\,\phi_{01}(x, 0), \tag{3.69}$$

equation (3.68) may be rewritten as

$$A = -2\int h_\mu \exp(-ik_0\mu)\,d\mu, \tag{3.70}$$

which is exactly the amplitude related to a pressure distribution $h(\mu)$ on a uniform current in deep water. Hence, in this interpretation, the Inui–Kajitani method is equivalent to solving the linearized problem for a modified pressure patch which is obtained from the original one by a co-ordinate straining given by (3.69). But this is precisely the procedure arrived at by the method of continuous mapping (§ 3.2), so that there is no difference in principle between our interpretations of the Guilloton and Inui–Kajitani methods, except for the forms of the straining, (3.42) and (3.69).

Although (3.70) has been derived for water of infinite depth, the extension to finite depth is straightforward. Thus, the potential ϕ_{01} has to satisfy the condition on the bottom (3.54), and (3.70) has to be replaced by

$$A = -\frac{2}{r}\int h_\mu \exp(-ik\mu)\,d\mu, \tag{3.71}$$

where k and r are given by (3.11) and (3.12), respectively.

4. Numerical results

4.1. *Choice of pressure distribution*

Following von Kerczek & Salvesen (1977), the pressure distribution used for the computations is defined as

$$\left.\begin{aligned} p(x) &= p_0 && \text{for} \quad |x| < \frac{L}{2} - e, \\ &= \tfrac{1}{2}p_0\left\{1 - \sin\left[\frac{\pi(|x| - L/2)}{2e}\right]\right\} && \text{for} \quad \frac{L}{2} - e < |x| < \frac{L}{2} + e, \\ &= 0 && \text{for} \quad |x| > \frac{L}{2} + e. \end{aligned}\right\} \tag{4.1}$$

The weight supported by the pressure, $W = p_0 L$, is independent of the smoothing parameter e.

This distribution is shown in figure 1, where it may be seen that its first derivative dp/dx is continuous and that it is zero at the ends. The smoothing parameter represents the length over which the pressure falls to zero and the relatively large value selected by von Kerczek & Salvesen for computational convenience was $e/L = 0{\cdot}25$.

4.2. *Comparison with numerical calculations*

In figures 2, 3 and 4 a series of comparisons are made between the four theories described here and some numerical computations of von Kerczek & Salvesen (1977). In their work, the Laplace equation was numerically solved in the flow region, and the position of the free surface was iterated until the dynamic condition was satisfied on it. The numerical procedures employed, in order to obtain the present results, are described in the appendix.

Figure 2 shows the results of perturbation theory for the three different Froude numbers for which detailed numerical results were given by von Kerczek & Salvesen (1977). The ordinate, $R/R_{1\infty}$, is the ratio of the resistance at the specified depth to the first-order resistance in deep water. The abscissa, h_0/L, is the dimensionless pressure-to-length ratio, that is, $p_0/\rho g L$. It is interesting to see how strong the nonlinear effects are in the case of finite depth – even for very low levels of the pressure. The linear result ($h_0/L = 0$) would indicate that the depths considered are almost equivalent to deep water. However, the depth factor plays a greater role as the pressure increases.

The second-order results (which appear as straight lines) are seen to be a great improvement on linear theory (which would be represented by a horizontal line at the value $R/R_{1\infty}$ corresponding to $h_0/L = 0$). The third-order results show almost perfect agreement for the range of pressures considered. Exceptions are the case of shallowest depth at $F = 0{\cdot}357$, and the case of deepest water at $F = 0{\cdot}302$. No explanation has been found for these two discrepancies.

The third-order results include the influence of speed correction given by (3.21), which was found to change the value of $R/R_{1\infty}$ by up to 5 %. In deep water, this effect was negligible for the pressures considered. Incidently, the *deep-water* perturbation calculations verify the results of von Kerczek & Salvesen – except for the third-order calculations at $F = 0{\cdot}357$.

The rather good agreement between the theory and the numerical results can probably be explained by the relative fineness of the pressure patch (the large value of

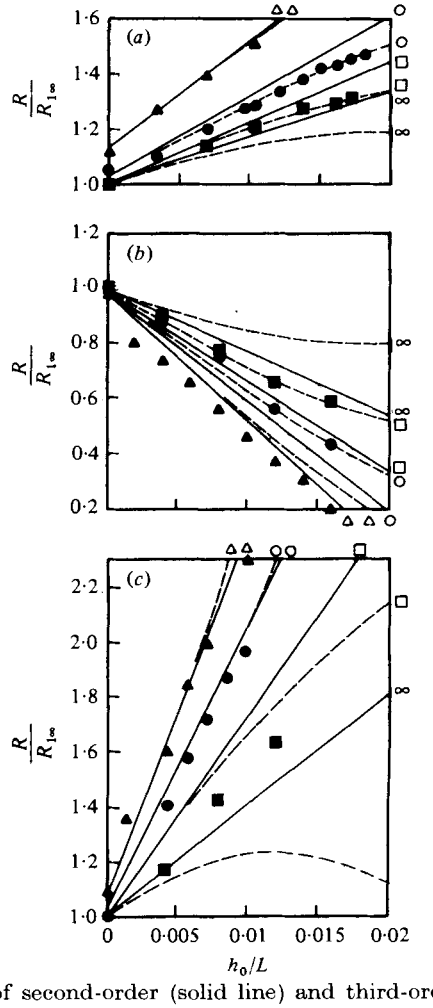

FIGURE 2. Comparison of second-order (solid line) and third-order (dashed line) perturbation theory with numerical results of von Kerczek & Salvesen (1977), $e/L = 0{\cdot}25$. (*a*) $F = 0{\cdot}461$, d/L values: △, 0·5714; ○, 0·7299; □, 1·0; ∞, ∞. (*b*) $F = 0{\cdot}357$, d/L values: △, 0·429; ○, 0·5; □, 0·625; ∞, ∞. (*c*) $F = 0{\cdot}302$, d/L values: △, 0·3012; ○, 0·3623; □, 0·5; ∞, ∞.

the smoothing parameter $e = 0{\cdot}25L$, and the fact that dp/dx is zero at the ends), which is not typical of air-cushion vehicles or ships.

The continuous-mapping theory (Guilloton) is examined in figure 3. The calculation has been done both with and without the pressure correction term of (3.49). The influence of this additional term is quite small. It may be seen that this theory displays the correct nonlinear trend, but in all cases the predicted degree of the nonlinearity is not sufficiently high – particularly in the case of $F = 0{\cdot}357$.

The theory is better at the two other Froude numbers of 0·461 and 0·302, where, in deep water at least, the outcome is almost identical to that of second-order perturbation theory.

Ideally, the continuous-mapping theory contains contributions from high-order terms, because of the implicit nature of the straining procedure. Nevertheless, the

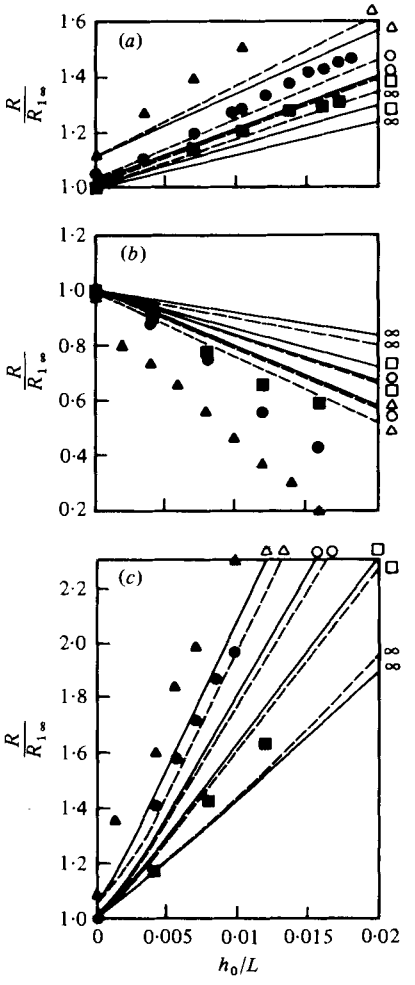

FIGURE 3. Comparison of continuous mapping theory (Guilloton) with pressure correction (solid line) and without (dashed line) with numerical results of von Kerczek & Salvesen (1977), $e/L = 0{\cdot}25$. (*a*) $F = 0{\cdot}461$, (*b*) $F = 0{\cdot}357$, (*c*) $F = 0{\cdot}302$. See figure 2 for symbols.

resulting curves are almost straight lines because of the low pressure levels used here and the smoothness of the distribution.

The two small-Froude-number theories are considered in figure 4. The approximation related to Baba & Takekuma's approach is seen to yield rather poor predictions. The degree of the nonlinearity is far too low, and even has the wrong trend at the intermediate Froude number of 0·357. As pointed out previously, the approximation may be obtained by replacing the first-order potential ϕ_1 by the zero-speed first-order potential ϕ_{01}, when computing the second-order pressure p_2. The loss of the waves and of the higher-order local terms from the first-order potential has a great influence on the results, and it may be concluded that this simplification is too great.

On the other hand, the Inui–Kajitani application of Ursell's theory predicts almost the correct degree of nonlinearity (figure 4). In deep water the results are practically identical to those of second-order perturbation theory. The principal difference

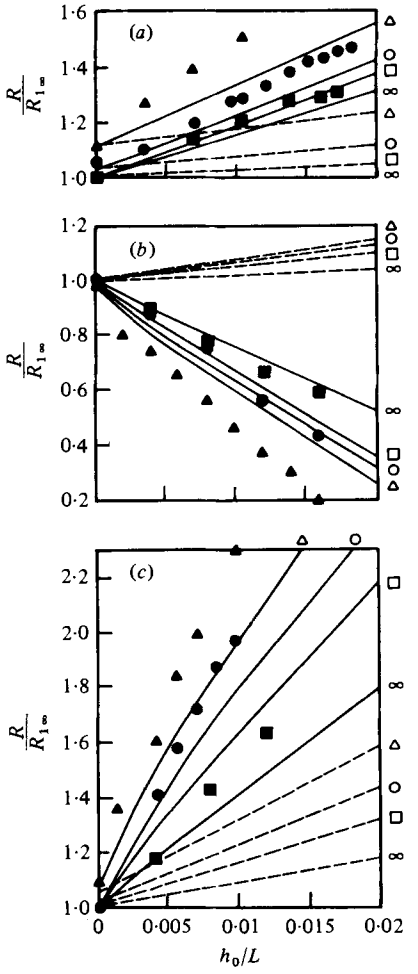

FIGURE 4. Comparison of Inui–Kajitani (solid line) and Baba & Takekuma (dashed line) small-Froude-number approximations with numerical results of von Kerczek & Salvesen (1977), $e/L = 0{\cdot}25$. (*a*) $F = 0{\cdot}461$, (*b*) $F = 0{\cdot}357$, (*c*) $F = 0{\cdot}302$. See figure 2 for symbols.

between the two theories considered in figure 4 is the method of handling the ϕ_{xx} term in the combined free-surface condition. Thus, in the Inui–Kajitani method, the waviness and higher-order local terms are neglected in the coefficient of ϕ_{xx} in (3.63) but not in ϕ_{xx} itself. It therefore would appear reasonable to take the zero-Froude-number approximation of the coefficient at least for the range of Froude numbers and pressures examined. On the other hand, we have shown that the Ursell theory as applied by Inui–Kajitani can be interpreted, like Guilloton's theory, as a continuous mapping which results in a straining of the pressure patch. Thus, from (3.27) and (3.42) we obtain for Guilloton's straining, by inverting (3.27), $X = x + \phi_1(x, 0)/c$, whereas (3.69) reads $\mu = x + (2/c)\,\phi_{10}(x, 0)$. It is seen, therefore, that the main difference between the two mappings, at least at moderate and low Froude numbers, is that Inui–Kajitani straining is twice Guilloton's and this has a beneficial effect on the accuracy of the results.

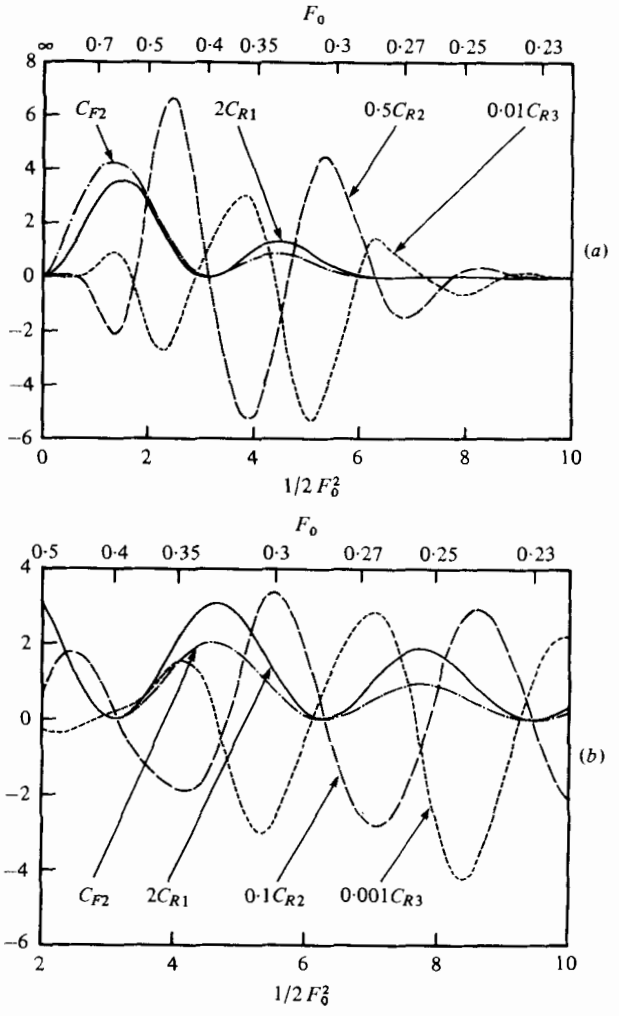

FIGURE 5. Wave-resistance and Froude-number correction coefficients from perturbation theory, $d/L = \infty$. (*a*) $e/L = 0{\cdot}25$, (*b*) $e/L = 0{\cdot}125$.

4.3. *Discussion of higher-order perturbation theory*

In the previous section the comparison between the numerical solution and the various approximations has been made for the three Froude numbers selected by von Kerczek & Salvesen (1977). Here, and in the following sections, we investigate the variation of the wave resistance based on the approximate theories for a broad range of Froude numbers, by using the numerical procedures given in the appendix.

The wave-resistance coefficients C_{Ri} and Froude-number correction coefficient C_{Fi} from perturbation theory are shown in figure 5, for two different degrees of pressure smoothing, $e/L = 0{\cdot}25$ and $e/L = 0{\cdot}125$, respectively. From these, the resistance may be computed in the following way:

$$C_R = C_{R1} + (h_0/L)\,C_{R2} + (h_0/L)^2 C_{R3} + \ldots, \tag{4.2}$$

and

$$F = F_0 + (h_0/L)^2 C_{F2} + \ldots. \tag{4.3}$$

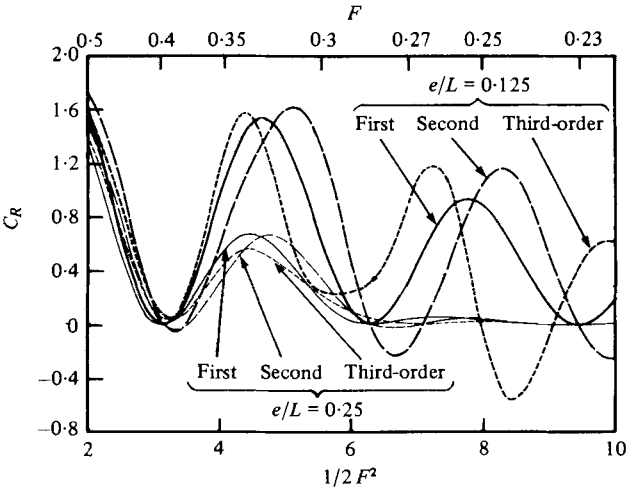

FIGURE 6. Influence of pressure smoothing on results of perturbation theory, $d/L = \infty$ and $h_0/L = 0{\cdot}02$.

The resistance coefficient is defined as follows,

$$C_R = \frac{R}{W} \cdot \frac{L}{2h_0}, \tag{4.4}$$

while the nominal Froude number is given by

$$F_0 = c_0/(gL)^{\frac{1}{2}}. \tag{4.5}$$

Both parts of figure 5 show that the second- and third-order contributions are oscillatory and that they are in phase but of opposite signs. Hence, the nonlinearity is weakened by the third-order term. The Froude-number correction is very small for the deep-water case under consideration. Equation (4.3) predicts a correction of about 0·0016 in the worst case when $h_0/L = 0{\cdot}02$. This correction does not occur at all in the development of three-dimensional higher-order theory because the wave pattern then dies out at infinity.

A further point of interest is that the higher-order resistance coefficients (C_{R2} and C_{R3}) in figure 5(*b*), unlike those of figure 5(*a*), have not begun to approach zero at the lowest Froude number considered. This feature implies that the theory would tend to break down at low speeds when the pressure distribution is sharper. This finding is in agreement with the analysis carried out by Dagan (1975) for a submerged body, which has shown that second-order nonlinear effects became relatively large at small Froude number, depending on the degree of bluntness of the leading edge.

The perturbation theory is examined further in figure 6, in which the usual wave resistance coefficient up to first, second, and third order is represented as a function of Froude number for the same two degrees of smoothing. A pressure level of $h_0/L = 0{\cdot}02$, which is typical of air-cushion vehicles, has been used. In the region, for which $F > 0{\cdot}4$, there is little difference between the theories of different order, and the influence of pressure smoothing is small.

However, for low Froude numbers, $F < 0{\cdot}27$, the influence of smoothing is indeed

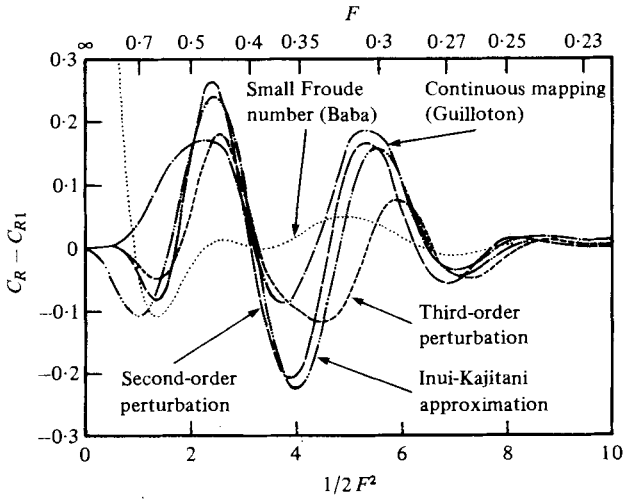

FIGURE 7. The nonlinear correction to the wave resistance according to the different theories, $e/L = 0{\cdot}25$, $h_0/L = 0{\cdot}02$, $d/L = \infty$.

marked. The greater smoothing is sufficient to almost completely damp the waves. The smaller smoothing has little influence.

The nonlinearity is very important for $F < 0{\cdot}4$ and results essentially in a shift of the wave-resistance curves. The second-order curves display a shift of the humps and hollows to lower Froude numbers, while the third-order ones indicate the opposite effect and reapproach the first-order curves. It may be emphasized that the shifting here is purely a result of changing values of the coefficients of resistance in (4.2). The Froude-number shift described by (4.3) is negligible in this case.

The breakdown of the theory at low Froude numbers, as evidenced by the negative resistance, is probably accompanied by wave breaking – a feature not modelled by the theory.

An interesting aspect of the nonlinearity, is that it appears to be very large when seen in figures 2, 3 and 4, for fixed Froude numbers, but less so here in figure 6, for fixed pressure loads. This feature results from the shifting of the humps and hollows which possess large slopes. This point was illustrated by von Kerczek & Salvesen.

Finally, one may observe that the second-order resistance becomes zero at those points where the first-order resistance is zero. This may be noted also from comparing (3.25*a*) and (3.25*b*), and this result represents a good check on the numerical procedure, since these equations were, in fact, not used for the calculation of the wave resistance itself.

4.4. *Comparison of the four different theories*

Finally, in figure 7, the nonlinear effect (that is, the difference between the resistance coefficient and the linear resistance coefficient) is plotted. The results of the four theories examined in the present study are presented for a dimensionless pressure of $p_0/\rho gL = 0{\cdot}02$. From the previous numerical comparisons, it would seem reasonable to assume that the third-order perturbation theory produces accurate results for the case at hand, and that it may be used for checking the other theories.

At low Froude numbers (less than 0·27) the continuous-mapping (Guilloton) and

second-order theories are quite close to each other. In the intermediate range ($0{\cdot}27 < F < 0{\cdot}35$), these two theories display the same phasing, but different magnitudes. At higher speeds still, the phasing is quite different.

For $F < 0{\cdot}27$, the Guilloton theory essentially agrees with the third-order theory, but is a little out of phase in the intermediate range ($0{\cdot}27 < F < 0{\cdot}35$). However, its magnitude in the intermediate range is better than that given by the second-order theory. At higher Froude numbers, greater than 0·35, the Guilloton and third-order theories can predict nonlinear corrections of opposite sign.

The Baba & Takekuma small-Froude-number theory is seen to predict a correction which is generally an order of magnitude too small. However, the weak oscillations in this curve do seem to be approximately in phase with the other curves. It should be pointed out here that the poor outcome of this theory led to a mistrust of the computer program. Nevertheless, the same results were obtained after the theory was programmed a second time, independently, by an assistant.

Finally, the Inui–Kakitani theory is seen to be very close in magnitude to the second-order theory over almost the entire range. In addition, the phasing is almost identical, being different by no more than 0·01 on the Froude-number scale.

5. Conclusions

The starting point of the present study was the numerical computation of the nonlinear wave resistance of the pressure distribution by von Kerczek & Salvesen (1977). In spite of the low value of the considered pressure-head to length ratio and the excessive smoothing of the distribution shape, the effect of the free-surface nonlinearity, for fixed Froude numbers and increasing pressure, is quite large. For instance, the ratio between the nonlinear and first-order wave resistance coefficients may reach the value of 0·2 in deep water for $h_0/L = 0{\cdot}01$ and $F = 0{\cdot}357$ (a near-hump Froude number). Computation of wave resistance for a broad range of Froude numbers and fixed pressure shows that the free-surface nonlinearity manifests itself mainly in a shift of the first-order wave-resistance curve, i.e. in a systematic change of the effective Froude number. The Froude number shift is, for instance, of order 0·01 for $F = 0{\cdot}3$ (figure 6, $h_0/L = 0{\cdot}02$, $e/L = 0{\cdot}125$), but this results in a relatively large change of the wave resistance at a given F because of the steep slope of the curve between a hollow and a hump ($\Delta C_R/\Delta F \cong 40$). This effect has been observed in previous studies (see, e.g., the survey of Tulin 1979) and it has far-reaching implications in the search for approximate theories and in applications.

The second-order consistent small-perturbation theory is shown to yield quite accurate predictions of the wave resistance at the three moderate-to-large Froude numbers considered by von Kerczek & Salvesen. The third-order results are practically indistinguishable from the numerical ones in most cases. This good agreement should not be surprising in view of the fineness of the pressure distribution shape. The small-Froude-number non-uniformity, discussed previously by Salvesen (1969) and Dagan (1975), does not show up because of the fast decay of the wave resistance for small F. Computations for a steeper pressure profile show, however, that the perturbation theory breaks down for small F and this agrees with the previous findings for submerged bodies by Dagan (1975). Speculating about application to ship wave resistance, it seems that higher-order perturbation theory may not be promising for displacement

ships which are not fine and which operate at relatively low F, the computational difficulties notwithstanding. In contrast, nonlinear effects are found to be small at high Froude numbers for large depth and there linear theory and small-perturbation expansions might be more useful.

Guilloton's method, in the interpretation of continuous mapping suggested by Noblesse & Dagan (1976), provides a nonlinear correction in the right direction, but of insufficient magnitude. It has the advantage of carrying out a change of the effective Froude number, thus avoiding the disastrous small-Froude-number non-uniformity mentioned above. Its partial success only, in quantitative terms, may be attributed to the neglect of the second-order terms in the field equations, which, by this indirect evidence, seem to be quite significant.

The small-Froude-number approximation of the type proposed by Baba & Takekuma (1975) for ships appears to be inadequate for predicting nonlinear wave resistance of a pressure distribution. It is reminded that unlike the quasi-linear original version of the theory by Ogilvie (1968), in which the coefficients of the velocity derivatives in the free-surface condition are expressed with the aid of the rigid-wall solution, in Baba's approximation the free-surface condition is linearized and the nonlinearity occurs in the presence of a non-homogeneous pressure term based on the rigid-wall solution. In the case of a fine pressure patch shape this non-homogeneous term can be expanded to second order in the pressure amplitude and then this small-Froude-number approximation turns out to be a degenerate case of the consistent perturbation theory. Replacing the first-order velocity derivatives by those of the zero-Froude-number solution in the second-order pressure terms is, therefore, inappropriate and leads to a considerable deterioration of results.

Finally, the application of Ursell's theory, of propagation of waves generated by a pressure point on a non-uniform current to ship waves as suggested by Inui & Kajitani (1977), leads to an improved prediction of nonlinear effects when compared with numerical or second-order perturbation theory. Since the starting point of the method is the quasi-linear free-surface condition proposed by Ogilvie (1968), it is inferred that the small-Froude-number approximation of (and only of) the coefficients of the velocity derivatives in the free-surface condition is sound. It should be mentioned, however, that Inui & Kajitani considerably simplify the theory, as compared with that of Ogilvie (1968) and Newman (1976), because they deal only with the propagation of the far free waves upon the slowly varying current represented by the rigid-wall solution, while the singularities which generate the waves are not modified by the free-surface presence. The present study casts additional light on the Ursell theory by showing that it can be equally interpreted, like Guilloton's theory, as a continuous mapping. Then it is seen to imply a horizontal straining of the pressure distribution by roughly twice the amount of Guilloton's displacement. This difference, and its beneficial effect upon prediction, is attributed to the attempt of Inui & Kajitani's method to satisfy, though only approximately, both free-surface and field equations at higher order, whereas Guilloton's straining is derived from the free-surface requirements solely.

Concluding, it seems that the studies of nonlinear wave resistance carried out in the last few years, including the present one, show that nonlinear free-surface effects are significant and they can be tackled by approximate theories which are manageable by the present and the next generation of computers. In principle, it seems that the nonlinearity of the free surface shows up as a phase-shift of the free waves by the velocity

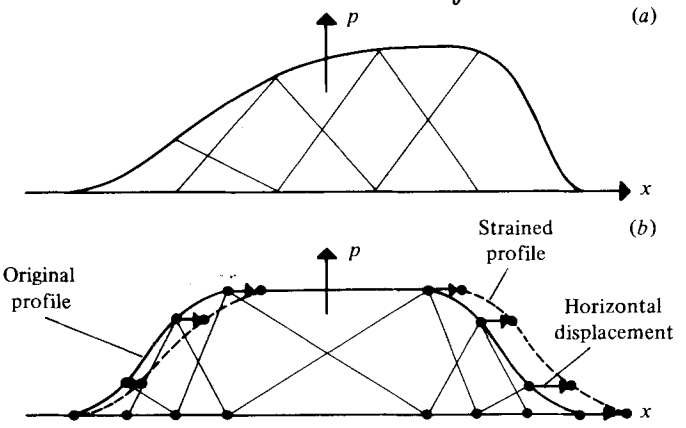

FIGURE 8. The numerical scheme: (*a*) use of overlapping triangles; (*b*) straining in the continuous-mapping theory (Guilloton).

field, rather than a change of their amplitude. Consequently, the modification of the wave resistance by nonlinear effects results from the interference of the far free waves (or, alternatively, their displacement along the body or the pressure patch), which in turn causes a shift of the resistance curve.

The work described in this paper was carried out while the first author was on sabbatical leave from the University of New South Wales, Sydney, Australia, at the University of Tel-Aviv, Israel. The opportunity is taken here for expressing his deep appreciation to both these institutions for their support.

Appendix. Numerical procedures

(*a*) *Perturbation theory*

The potentials ϕ_i induced by each of the pressure distributors p_i given by (3.14), (3.18) and (3.22) were computed successively, starting from the first. For this purpose, the distribution was broken into a series of overlapping triangles as shown in figure 8(*a*). Thus, the pressure curve was modelled by a series of straight-line segments. For a typical triangle of strength p_i, whose vertices are located at x_1, x_2 and x_3, we may integrate (3.9) to give its contribution $\Delta\phi_i$ to the potential on the undisturbed free surface:

$$\Delta\phi_i(x,0) = \frac{\hat{p}_i}{\rho c}\left\{\frac{1}{x_2-x_1}[Z(x-x_2)-Z(x-x_1)]-\frac{1}{x_3-x_2}[Z(x-x_3)-Z(x-x_2)]\right\}, \quad (A\,1)$$

where Z is given by

$$Z(x) = \frac{1}{\pi}\left[\int_0^\infty \left(\frac{\sin(kx)}{k^2q(k)}-\frac{x}{k^2(1-k_0d)}\right)dk-\frac{\pi\cos(k_1x)}{k_1^2r(k_1)}\right]. \quad (A\,2)$$

A second term has been added to the integral in (A 2). It has the property of removing the singularity in the integrand at $k = 0$ without affecting $\Delta\phi_i$ in (A 1).

The range of the integral in (A 2) was broken at the point $k = k^*$, at which

$$\tanh(k^*d) = 0{\cdot}99999.$$

The integral from 0 to k^* was performed numerically, while that from k^* to ∞ was

carried out analytically. When the singularity occurred in the first integral, that is $0 < k_1 < k^*$, then the singular part was extracted from the numerical computation. The integration mesh was automatically refined until an absolute error of 0·00001 was achieved. The function (A 2) only has to be computed once for each Froude number, for a single set of (equally spaced) x values.

The first-order potential ϕ_1 was then calculated using (A 1). From this, ζ_1 and p_2 were found from (3.6a) and (3.18), respectively. For this purpose, derivatives of the potential are needed. Derivatives with respect to x were done numerically using standard difference formulae. Derivatives with respect to y on (A 1) are not possible in a direct way. Instead, ϕ_{1y} was found from (3.8), and the relation $\partial^2/\partial y^2 = -\partial^2/\partial x^2$ from (3.4) was used to evaluate the second y derivative.

The second-order and third-order potentials were found in a similar way using (A 1), (3.8) and (3.6b), and then (3.22), (A 1), (3.8) and (3.6c), respectively. The wave-resistance contributions from each of the three orders were evaluated from (3.26).

The pressure distributions p_2 and p_3 (3.18) and (3.22) were truncated at a distance of one free wavelength beyond the pressure patch p_1, while the mesh spacing used was $0{\cdot}01875L$. These parameters and the error parameters mentioned previously were found to result in a relative error in the resistance of less than 1 %.

(*b*) *Continuous-mapping theory*

The numerical procedure for evaluating this theory was divided into two stages. The main stage is the straining of the co-ordinate system given by (3.44), this being an implicit definition.

The pressure patch was represented by a set of equally spaced triangles over the ends of the patch, where the pressure varies. In the central region, where the pressure is constant, only two asymmetrical triangles were needed. This is illustrated in figure 8(*b*). The iteration procedure started with the evaluation of the potential Φ, using (A 1), and then the straining ξ_1, from (3.44). The x co-ordinate was then stretched using (3.27), and the straining evaluated again. For this iteration and later ones, all the pressure triangles will be asymmetrical, but (A 1) is quite general. However, to save computing time, the function (A 2) was evaluated only once, and parabolic interpolation was used to obtain values of Z, at arbitrary points.

The iteration procedure was repeated until the straining no longer changed, and the downstream wave amplitude was calculated from (3.13).

As explained in § 3.2, the present problem requires the evaluation of an additional second-order downstream wave from (3.49), which does not occur in the usual ship problem. The effect may be represented by a pressure gradient given by

$$p_{2x} = -\frac{1}{c}(pu_1)_x + \frac{1}{\pi\rho g}\int_{-\infty}^{\infty} [p_s^2 - \rho c(pu_{1s})_s + pp_{ss}]\frac{ds}{s-x}. \tag{A 3}$$

The downstream wave may now be found from (3.13) and (3.10). The integration in (3.10) is done before that in (A 3). The effect of finite depth on the integral may be accounted for in the usual way by including reflexions spaced $2d$ apart in the y direction. After some algebra, the following result may be obtained,

$$A_2 e^{i\alpha_2} = \frac{2}{\rho g c r(k_1)}\int_{-\infty}^{\infty} p(v_1 k_0 - iu_1 k_1)\exp(iks)\,ds. \tag{A 4}$$

This wave was added to that induced by the strained first-order pressure. The wave resistance was then calculated from (3.25).

In the numerical work a spacing in the argument of the Z function was chosen to be $0{\cdot}01L$, and the iteration procedure was stopped when the largest strain change was less than $0{\cdot}00001L$. The method usually converged after 3 or 4 steps. (The straining for one nominal pressure $p_0/\rho gL$ was used as the starting point for the next one, which was typically chosen to increase in steps of 0·005.) The resulting absolute error in the resistance coefficient was about 0·001.

(*c*) *Small-Froude-number approximation (Baba & Takekuma approximation)*

The resistance in this theory was evaluated through the downstream waves from (3.13) and (3.10) using the equivalent pressure distribution in (3.61). Each term in (3.61) is a trivial function of the pressure distribution (4.1), with the exception of the function ϕ_{01x}.

Since ϕ_{01x} is an analytic function within the fluid, it may be expressed in terms of ϕ_{01y} around the border, using (3.58). If one includes the effect of the bottom by means of reflexions, the result is

$$\phi_{01x} = \frac{c}{\pi\rho g} PV \int_{-\infty}^{\infty} p_s \left(\sum_{n=-\infty}^{\infty} \frac{1}{s-x+2ind} \right) ds. \tag{A 5}$$

The integration may be performed analytically to give

$$\phi_{01x} = \frac{cp_0}{4\rho ge} \sum_{n=-\infty}^{\infty} [f(\beta_1)+f(\beta_2)-f(\beta_3)-f(\beta_4)], \tag{A 6}$$

where

$$\left.\begin{aligned} \beta_1 &= -\frac{\pi}{2}\left(\left(x+\frac{L}{2}\right)\Big/ e-1\right)+\lambda_n, \\ \beta_2 &= -\frac{\pi}{2}\left(\left(x+\frac{L}{2}\right)\Big/ e+1\right)+\lambda_n, \\ \beta_3 &= -\frac{\pi}{2}\left(\left(x-\frac{L}{2}\right)\Big/ e-1\right)+\lambda_n, \\ \beta_4 &= -\frac{\pi}{2}\left(\left(x-\frac{L}{2}\right)\Big/ e+1\right)+\lambda_n \end{aligned}\right\} \tag{A 7}$$

and

$$\lambda_n = i\pi nd/e. \tag{A 8}$$

The special function f is one of the two auxiliary functions for the cosine and sine integral defined by Abramowitz & Stegun (1965, p. 232):

$$\left.\begin{matrix} f(z) \\ g(z) \end{matrix}\right\} = \int_0^{\infty} \frac{\begin{matrix}\sin \\ \cos\end{matrix}(t)}{x+t}\, dt. \tag{A 9}$$

These functions may be expressed as follows:

$$f(z) = \frac{i}{2}[I(iz)-I(-iz)], \quad g(z) = \tfrac{1}{2}[I(iz)+I(-iz)], \tag{A 10}$$

where

$$I(z) = e^z E_1(z). \tag{A11}$$

Here E_1 is the exponential integral defined by Abramowitz & Stegun (1965, p. 230). The f and g functions were computed from (A 10) using a numerical approximation for $I(z)$ given by Hess & Smith (1967).

Examination of (3.61) and (A 6) shows that the equivalent pressure can be decomposed into terms independent of p_0 and c (except for simple multiplying factors), so that the computer program can be made very efficient. The infinite sum in (A 6) was truncated at $n = \pm 32$, and the distribution (3.61) which theoretically extends to infinity was cut off at $x = \pm L$. The pressure was then represented by 80 equally spaced overlapping triangles, as in the other methods. The resulting error in the wave resistance coefficient was about 0·5 %.

(*d*) *Inui–Kajitani approximation*

The resistance was computed by means of the downstream wave amplitude using (3.25*a*), (3.13) and (3.10), on the basis of a strained pressure distribution, defined by (3.72). The straining function is seen to be essentially the integral of (A 6) with respect to x. That is:

$$\xi = \frac{2}{c}\phi_{01} = \frac{p_0}{\pi\rho g}\sum_{n=-\infty}^{\infty}[-G(\beta_1)-G(\beta_2)+G(\beta_3)+G(\beta_4)], \tag{A 12}$$

in which

$$G(z) = g(z)+\ln(z), \tag{A 13}$$

and the arguments of the functions are given by (A 7).

The straining (A 12) need only be computed once for a set of values of p_0 and c. The overlapping triangles used to model the pressure were distorted along with the straining, as in figure 8 (*b*). A choice of 40 such triangles at each end of the distribution was made (because the pressure is constant in the middle portion, only two were used there). The infinite sum in (A 12) was truncated at $n = \pm 32$. This resulted in a relative error of about 0·1 %.

REFERENCES

Abramowitz, M. & Stegun, I. A. 1965 *Handbook of Mathematical Functions*. Washington: National Bureau of Standards.

Baba, E. & Takekuma, K. 1975 A study on free-surface flow around bow of slowly moving full forms. *J. Soc. Nav. Arch. Japan* **137**, 1–10.

Dagan, G. 1972 Nonlinear ship wave theory. *Proc. 9th Symp. on Naval Hydrodynamics, Paris*, pp. 1697–1737. Office of Naval Research.

Dagan, G. 1975 Waves and wave resistance of thin bodies moving at low speed: the free surface nonlinear effect. *J. Fluid Mech.* **69**, 405–417.

Gadd, G. E. 1973 Wave resistance calculations by Guilloton's method. *Trans. Roy. Inst. Naval Arch.* **115**, 377–384.

Guilloton, R. 1964 L'étude théorique du bateau en fluide parfait. *Bull. Assoc. Tech. Maritime Aero.* **64**, 537–552.

Hess, J. L. & Smith, A. M. O. 1967 Calculation of potential flow about arbitrary bodies. *Progress in Aeronautical Science*, vol. 8, pp. 1–138. Pergamon.

Inui, T. & Kajitani, H. 1977 A study on local nonlinear free surface effects in ship waves and wave resistance. *25th Anniv. Coll. Inst. für Schiffbau, Hamburg.*

Kerczek, C. von & Salvesen, N. 1977 Nonlinear free-surface effects – the dependence on Froude number. *Proc. 2nd Int. Conf. on Numerical Ship Hydrodynamics, Berkeley.*

Newman, J. N. 1976 Linearized wave resistance theory. *Proc. Int. Seminar on Wave Resistance, Tokyo.* Soc. Naval Architects of Japan.

Noblesse, F. & Dagan, G. 1976 Nonlinear ship-wave theories by continuous mapping. *J. Fluid Mech.* **75**, 347–371.

Ogilvie, T. F. 1968 Wave resistance – the low speed limit. *Dept. of Naval Arch. & Mar. Engng Rep.* 002. University of Michigan.

SALVESEN, N. 1969 On higher-order wave theory for submerged two-dimensional bodies. *J. Fluid Mech.* **38**, 415–432.

SALVESEN, N. & KERCZEK, C. VON 1976 Comparison of numerical and perturbation solutions of two-dimensional nonlinear water-wave problems. *J. Ship Res.* **20**, 160–170.

TUCK, E. O. 1965 The effect of nonlinearity at the free surface on flow past a submerged cylinder. *J. Fluid Mech.* **22**, 401–414.

TULIN, M. P. 1979 Ship wave resistance – a survey. *Proc. 8th Nat. Cong. of Appl. Mech. U.S.A.* (in the press). [Also *Hydronautics, Inc. Rep.* (in the press).]

URSELL, F. 1960 Steady wave patterns on a non-uniform steady flow. *J. Fluid Mech.* **9**, 333–346.

WEHAUSEN, J. V. 1973 The wave resistance of ships. *Adv. Appl. Mech.* **13**, 93–245.

WEHAUSEN, J. V. & LAITONE, E. V. 1960 Surface waves. *Encyclopedia of Physics*, vol. 9 (ed. S. Flügge), pp. 446–778. Springer.